SCIENCE CHINA Materials

ARTICLES

mater.scichina.com link.springer.com

Published online 30 September 2015 | doi: 10.1007/s40843-015-0090-x
Sci China Mater 2015, 58: 811–818

Preparation and adsorption capacity evaluation of graphene oxide-chitosan composite hydrogels

Heng Zhao[1], Tifeng Jiao[1,2,3*], Lexin Zhang[1], Jingxin Zhou[1], Qingrui Zhang[1*], Qiuming Peng[2] and Xuehai Yan[3]

Graphene oxide (GO)-chitosan composite hydrogels were successfully prepared via the self-assembly of chitosan molecules and GO. These as-prepared hydrogels were characterized by different techniques. The morphology of the internal network structure of the nanocomposite hydrogels was investigated. The adsorption capacity results demonstrate that the prepared GO-based composite hydrogels can efficiently remove three tested dye molecules, Congo red, methylene blue and Rhodamine B, from wastewater in accordance with the pseudo-second-order model. The dye adsorption capacity of the obtained hydrogels is mainly attributed to the GO sheets, whereas the chitosan molecule was incorporated to facilitate the gelation process of the GO sheets. The present study indicates that the as-prepared composite hydrogels can serve as good adsorbents for wastewater treatment as well as the removal of harmful dyes.

INTRODUCTION

Graphene has been attracting a lot of interest in diverse fields, such as chemistry, materials, physics, energy, and fuels, since the first report on its preparation via mechanical exfoliation [1–6]. Graphene oxide (GO), a kind of highly oxidized and chemically modified graphene material, contains various functional groups, such as hydroxyls, epoxides, and carboxyls in plane or at the edge. The surrounding carboxylate group can improve colloidal stability and negative interfacial charge distribution [7], while the hydroxyl and epoxide functional groups in plane can interact via noncovalent interaction, such as hydrogen bonding and π-π stacking [8]. These special characteristics make GO a potential adsorbent material. Therefore, various GO-based adsorbent materials have been developed to facilitate the separation of dye or poison from aqueous solutions [9–12]. In addition, three-dimensional (3D) porous gels from graphene composites show new properties, such as large surface areas, high compressibility, ultralow density, and strong mechanical strength [13–16]. For example, Banerjee *et al.* [17,18] successfully achieved the preparation of various hydrogels that can be used as dye-adsorbing agents in waste-water removal. In addition, this group has also reported metal-nanoparticle-containing GO-based hydrogels and novel morphological transformation of graphene based nanohybrids [19–21]. Generally, GO-based composite hydrogels were obtained by mixing organic macromolecules or small amphiphiles with an aqueous GO dispersion [22–24]. Chitosan (CS), a well-known compound of chitin *N*-deacetylation, shows many eco-friendly properties, such as biodegradation, good biocompatibility, and antifungal activity. These characteristics make it a promising candidate in the fields of catalysis, materials, food, drugs, etc. [25–27]. Since GO crosslinks with chitosan via the carboxyl, hydroxyl, epoxy, and amine groups of chitosan, the adsorption capacity of the formed composite is expected to be high. To date, some reports have been published on GO-chitosan nanocomposites used for drug release and antimicrobial activity [28–32].

In this study, we report the preparation of GO-based composite hydrogels using the self-assembly of CS and GO, and an *in situ* reduction approach. The composite hydrogels consist of both hydrogen bonding and electrostatic interactions between the CS molecules and GO sheets. CS molecules were incorporated to facilitate the gelation process of GO sheets, and the dye adsorption capacity of the hydrogel was mainly attributed to the GO sheets. For the three dyes tested in this study, namely, Congo red (CR), methylene blue (MB), and Rhodamine B (RhB), the as-prepared composite hydrogels exhibit good removal rates in accordance with the pseudo-second-order model. More importantly, the hydrogels prepared in this study have potential large-scale applications in organic dye removal and

[1] Hebei Key Laboratory of Applied Chemistry, School of Environmental and Chemical Engineering, Yanshan University, Qinhuangdao 066004, China
[2] State Key Laboratory of Metastable Materials Science and Technology, Yanshan University, Qinhuangdao 066004, China
[3] National Key Laboratory of Biochemical Engineering, Institute of Process Engineering, Chinese Academy of Sciences, Beijing 100190, China
* Corresponding authors (emails: tfjiao@ysu.edu.cn (Jiao T); zhangqr@ysu.edu.cn (Zhang Q))

wastewater treatment.

EXPERIMENTAL DETAILS

Materials

CS (>90% degree of deacetylation) was purchased from Sinopharm Chemical Reagent Co., Ltd (Beijing, China). CR, RhB, and MB were obtained from Tianjin KaiTong Chemical Reagent co., Ltd (Tianjin, China). Other materials, such as sulfuric acid (98%), vitamin C, potassium permanganate ($KMnO_4$), graphite powder (99.85% purity), hydrogen peroxide (30%, *w*/*w*), potassium nitrate (KNO_3), and hydrochloric acid, were obtained from Aladdin Chemicals (Tianjin, China) and used without further purification. The water used in all the experiments was obtained using a Milli-Q ultrapure water purification system.

Fabrication of the GO/CS and reduced GO/CS hydrogels

GO was obtained from graphite powder according to a modified Hummers method [33]. Brown GO sheets were obtained after centrifugation and freeze-drying at −50°C for 2−3 days. GO-based composite hydrogels, including GO/CS hydrogel and reduced GO (RGO)/CS hydrogel, were prepared using CS. In a typical experiment, 4.0 mL of an aqueous dispersion of GO (5 mg/mL) was mixed with 0.4 mL of CS (30.0 mg/mL, prepared in 2.5% acetic acid (HAc) solution) in a glass vial. In order to obtain a homogeneous gelation state, the hydrogel was then sonicated for 2−3 min. For the preparation of the RGO/CS composite hydrogel, 1.0 mL of vitamin C solution (60 mg/mL) was first added into 4.0 mL of a GO aqueous dispersion (5 mg/mL), which was stirred for several minutes. Next, 0.4 mL of CS (30.0 mg/mL, prepared in 2.5% HAc solution) was added to the above solution and the obtained ternary mixture was sonicated for about 10 min and heated subsequently at 90°C for 10 min. After heating, the GO component in the gel transformed to RGO with slight shrinking of the gel state.

Adsorption experiments

Adsorption capacity experiments were designed and modified according to previous reports [34,35]. In adsorption experiments, about 1 mL of GO/CS or RGO/CS hydrogels (without lyophilization) was added to 100 mL of each dye solution (MB, 10 mg/L; RhB, 5 mg/L; CR, 5 mg/L). These solutions were slowly stirred in dark at a constant rate at room temperature. Supernatant liquid was withdrawn at different time intervals for subsequent characterization using an UV-vis spectrometer (752, Sunny Hengping, Shanghai, China). Different absorbance wavelengths (662 nm for MB, 554 nm for RhB, and 497 nm for CR) were utilized to determine the concentration of the residual dyes in the supernatant liquid.

Characterization

The GO sheets and xerogels used in the present study were prepared using a lyophilizer at −50°C with a FD-1C-50 lyophilizer instrument from Beijing Boyikang Experimental Instrument Co., Ltd. (Beijing, China) for more than 2 days. The nanostructures of all the lyophilized samples were studied by a field-emission scanning electron microscope (SEM) (S-4800II, Hitachi, Japan) with 5−15 kV accelerating voltage as well as a transmission electron microscope (TEM) (HT7700, Hitachi High-Technologies Corporation, Japan). Thermogravimetry-differential scanning calorimetry (TG-DSC) characterizations were carried out by using a NETZSCH STA 409 PC Luxxsi multaneous thermal analyzer (Netzsch Instruments Manufacturing Co., Ltd., Germany) in air. X-ray diffraction (XRD) was conducted on an X-ray diffractometer equipped with a Cu Kα X-ray radiation source and a Bragg diffraction setup (SMART LAB, Rigaku, Japan). Raman spectroscopy was performed on a Horiba Jobin Yvon Xplora PLUS confocal Raman microscope equipped with a motorized sample stage. The wavelength of the excitation laser was 532 nm and the laser power was maintained below 1 mW without noticeable sample heating.

RESULTS AND DISCUSSION

Structure characterization of hydrogels

The photographs of the GO aqueous solution, GO/CS gels, and RGO/CS composite gels are demonstrated in Fig. 1f. It indicates that both gels show good gelation stability. Both the SEM and TEM pictures of the obtained composite hydrogels in Fig. 1 indicate that porous 3D network nanostructures were formed by the self-assembly of GO sheets and CS molecules. It should be noted that after *in situ* reduction of GO by vitamin C under heating (90°C), the GO composite gel can transform to an RGO-based hydrogel. It is well known that vitamin C usually acts as an eco-friendly moderate reducing agent. At the same time, the formed composite gels can provide enough space among its 3D nanostructure for the adsorption of organic dyes.

In addition, XRD was used to characterize the obtained organized nanostructures in the composite materials, as shown in Fig. 2. For the GO sheet and lyophilized GO/CS hydrogel samples, the peaks that appear at 11.1° and 9.8°, respectively indicate increased layer spacing between the GO layers in the organized composite gels. In the XRD pat-

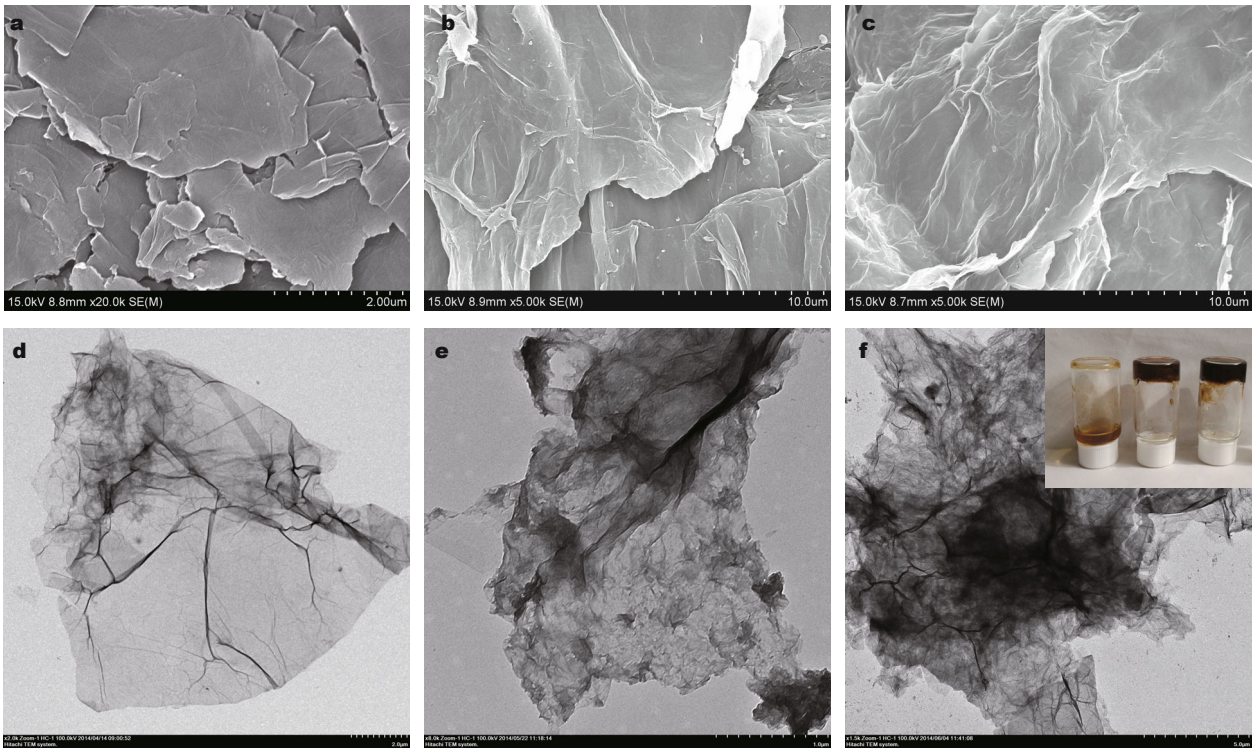

Figure 1 SEM and TEM images of GO sheet (a, d), GO/CS hydrogel (b, e), and RGO/CS hydrogel (c, f), respectively. The inset in image f shows the GO aqueous solution and both composite hydrogels (left to right).

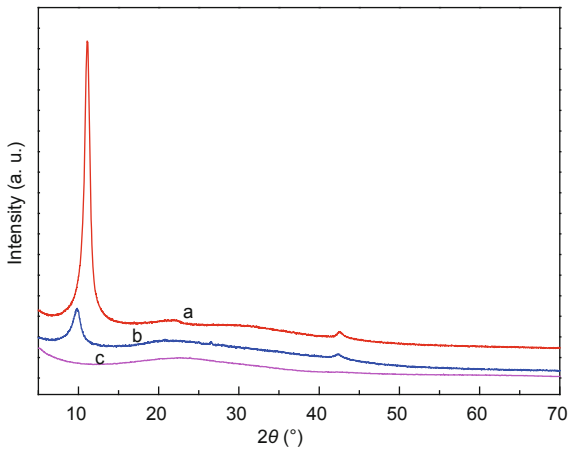

Figure 2 XRD patterns of the obtained samples: a, GO sheet; b, GO/CS gel; c, RGO/CS gel.

tern of the dried RGO composite hydrogel, a broad peak centered at 2θ = 22.6° is clearly seen and the diffraction peak at 2θ = 11.1° in the GO gel disappears. This change suggests that the transformation from GO to RGO is accompanied by the removal of various oxygen-containing functional segments on the GO surface [36].

Fig. 3a illustrates the thermograms of the obtained composite gel materials. It can be concluded from the TG data that both the composite hydrogels demonstrate better thermal stability compared with GO; this could mainly be due to the self-assembly and cross-linked nanostructures in the gels. The data indicates two obvious mass loss peaks at around 200 and 500°C for the composite materials; these mainly originate from the pyrolysis of the oxygen-containing segments in the GO sheets and CS molecules, respectively. At temperatures higher than 560°C, no further change is observed in the mass of the prepared RGO gel material. GO composites have been previously reported to demonstrate various weight retention ratios at a high temperature range, mainly due to the change in the self-assembly of the 3D porous carbon composites [37]. In the present study, the as-prepared composite materials clearly exhibit enhanced thermal stability in comparison with pristine GO.

It is well known that Raman spectroscopy is a useful technique to investigate various carbon composite materials [38]; the Raman spectra for the composites are shown in Fig. 3b. The spectrum shows three obvious bands at 1601 cm^{-1}, 1351 cm^{-1}, and 2692 cm^{-1}, which can be assigned to the G band, D band, and 2D band, respectively

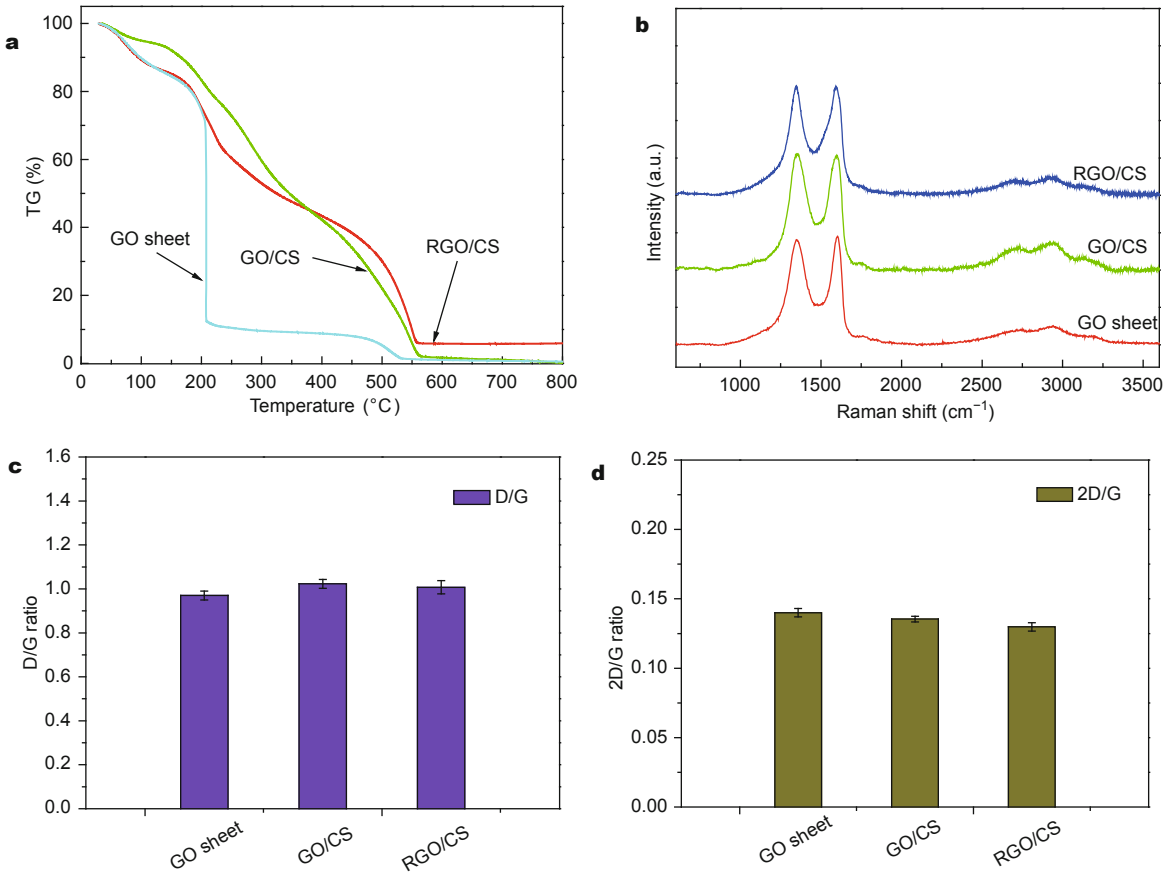

Figure 3 TG curves (a) and Raman spectra (b) of the obtained lyophilized samples. (c) and (d) show the calculated D/G and 2D/G ratios in Raman spectra from (b).

[39,40]. It has been reported that the G and 2D bands can shift to lower and higher wavenumbers from their original positions at 1585 and 2679 cm^{-1}, respectively, when single-layer graphene sheets are transformed to the multilayer (about 2–6 layers) state [41,42]. On the other hand, the 2D/G ratios for graphene sheets with different layers (1, 2, 3, >4) are normally >1.6, 0.8, 0.30, and 0.07, respectively [43,44]. Recently Akhavan and co-workers [45] have reported single and bilayer GO sheets with 2D/G ratios in the range of 1.53–1.68 and 0.82–0.89, respectively. For the present study, the 2D/G ratios in both the composite materials were calculated to have values ranging from 0.11 to 0.14, shown in Fig. 3d, indicating that the as-prepared graphene samples possessed multilayer structures. Furthermore, it is also well known that the D/G peak intensity ratio can serve as a characteristic of the sp^2 area size of graphene sheets containing sp^3 and sp^2 bonds. In the present case, the results indicate that the D/G ratio changes from 0.97 to 1.02–1.14 after the self-assembly in composite gels, as seen in Fig. 3c.

Adsorption capacity of hydrogels

The dye adsorption capacity of the as-prepared composite hydrogels was investigated by placing the obtained composite gel materials in aqueous CR, MB, and RhB solutions, respectively. It should be noted that the adsorption process of the freeze-dried samples seemed typical and easy to investigate. In present work, we investigated the *in situ* adsorption capacity of hydrogels, which could demonstrate the real adsorption process of GO-based gels for different dyes in wastewater. In addition, GO-based composites may act as a potential photocatalyst for degradation of dyes under visible light condition. The present adsorption experiments were measured and repeated under dark conditions to avoid this effect of GO as catalyst. Different absorbance wavelengths (497 nm for CR, 662 nm for MB, and 554 nm for RhB) were utilized to investigate the residual dye concentrations at various time intervals. At the same

time, the dye removal rates were calculated according to the equation: $K = (A_0 - A_T)/A_0 \times 100\%$, where K is defined as the dye removal rate, A_0 is defined as the absorbance of the dye solution, and A_T is defined as the absorbance of the supernatant liquid collected at different intervals. Fig. 4 plots the dye removal rate as a function of time for the three dyes. The dye removal rates reach stable values for both MB and RhB within approximately 20 min, suggesting that the as-prepared composite hydrogels act as efficient dye adsorbents. In addition, the thermodynamic behaviors of the other RGO-based hydrogels for dye adsorption capacity have been characterized in detail [46]. We performed primary adsorption kinetic experiments of the as-prepared composite hydrogels on different dyes, and the obtained data are shown in Fig. 5. The hydrogels demonstrated continuous and homogeneous adsorption, with equilibrium times of around 50 min for CR and 20 min for MB and RhB, respectively. The obtained kinetic results can mainly originate from the prepared special 3D porous nanostructures by electrostatic force and hydrogen bonding, as well as highly dispersed GO nanosheets as adsorption substrates. It should be noted that classical kinetic models were used to explain the adsorption process as follows:

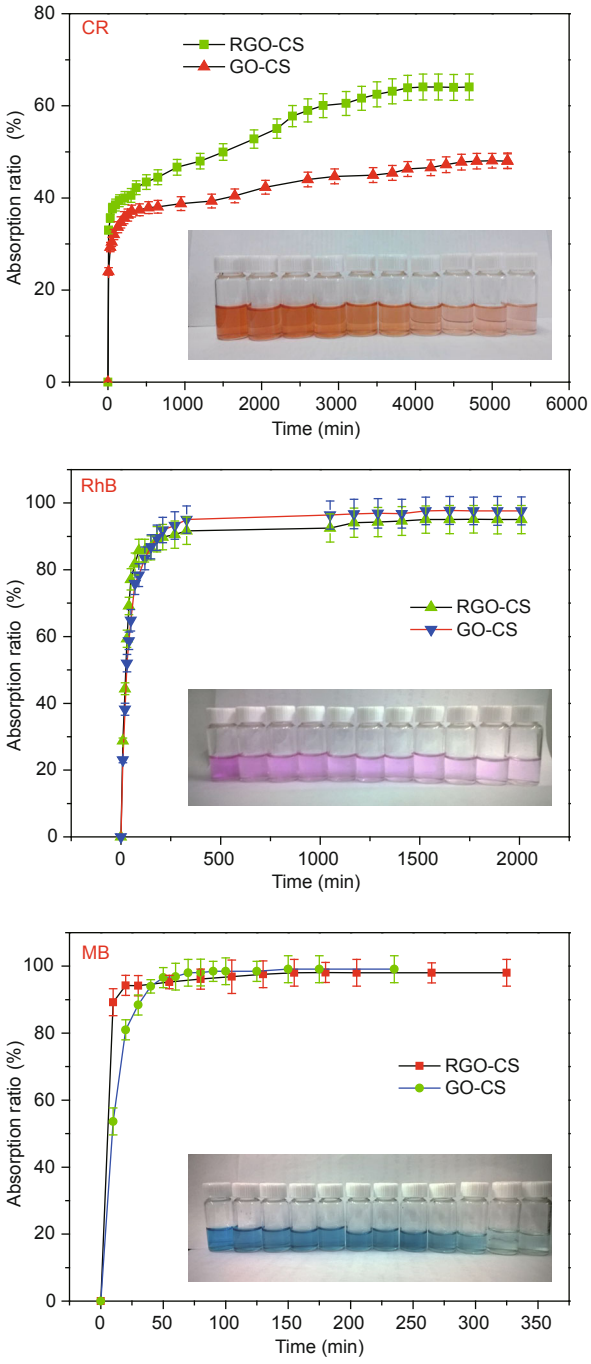

Figure 4 Adsorption properties of GO/CS and RGO/CS hydrogels for the three dye solutions used. The inserted pictures show the colorful dye solutions obtained from supernatant liquids at different time intervals.

The pseudo-first-order model:

$$\log(q_e - q_t) = \log q_e - \frac{k}{2.303}t \,. \quad (1)$$

The pseudo-second-order model:

$$\frac{t}{q_t} = \frac{1}{kq_e^2} + \frac{t}{q_e} \,, \quad (2)$$

where q_e and q_t are defined as the adsorbed dye amount (mg/g) at equilibrium and time t, respectively, and k_1 and k_2 represent the kinetic rate constants [10–12]. From the kinetic data in Table 1, it can be concluded that the adsorption process in all cases is in accordance with the pseudo-second-order model with good correlation coefficient ($R^2 > 0.999$ for MB and RhB, $R^2 > 0.992$ for CR). Considering the obtained experimental results described above, it should be noted that the present composite hydrogels are more environmentally friendly than organogels prepared from different organic solvents [47–49]. Detailed studies on the drug release behaviors and the preparation of nanoparticle-containing hybrid hydrogels using the present supramolecular gels are still underway.

CONCLUSIONS

In summary, we reported the preparation of two GO/CS composite hydrogel materials and evaluated their adsorption capacity for three different dyes. The CS molecule was chosen for its functional amine segments in the molecular skeleton that can form porous gel nanostructures via interactions such as hydrogen bonding. Morphological characterizations of the obtained gel materials demonstrate the formation of porous 3D nanostructures by a self-assembly

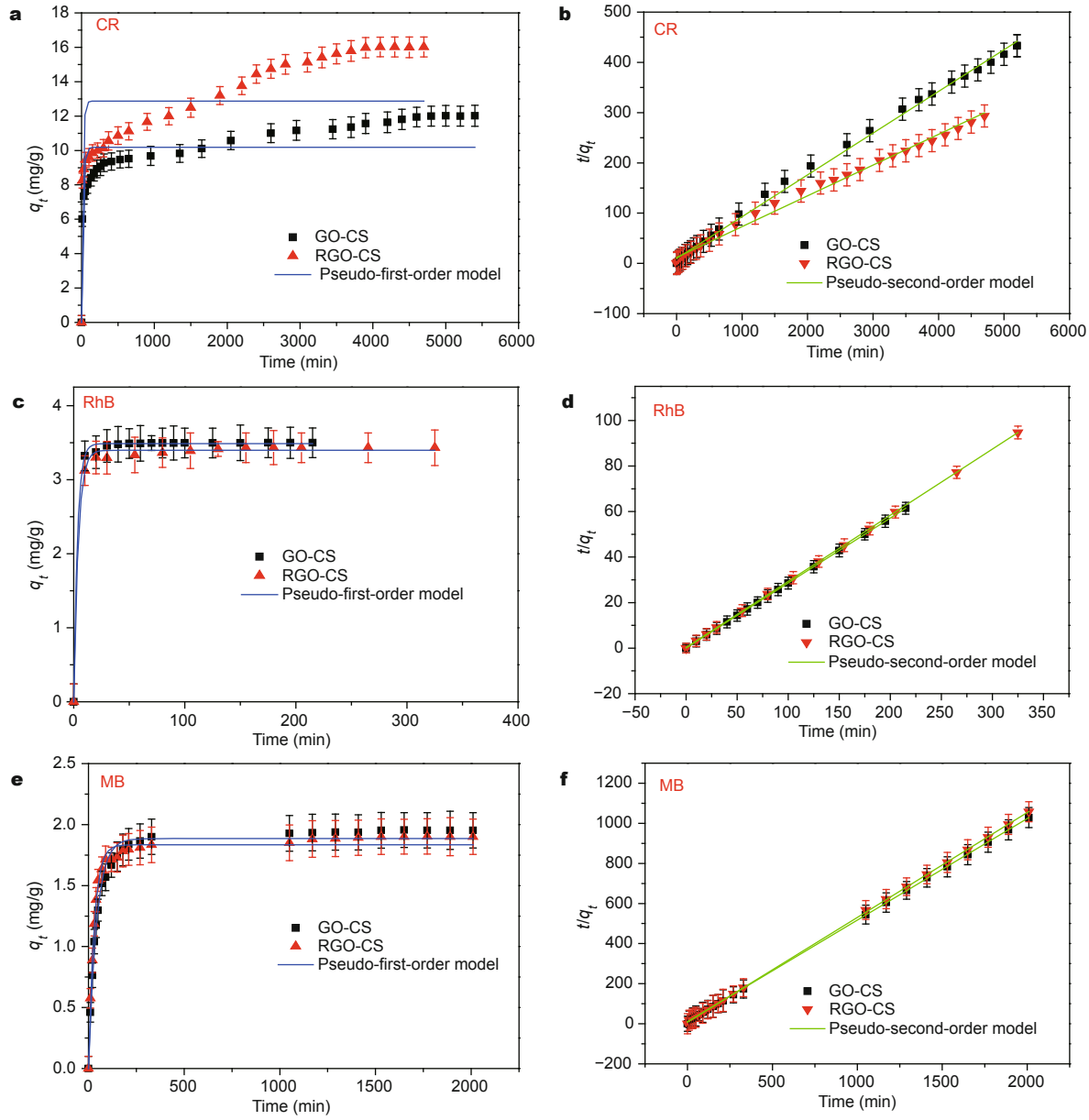

Figure 5 Adsorption kinetics curves of GO/CS and RGO/CS hydrogels for different dye adsorptions: (a, c, e) pseudo-first-order kinetics; (b, d, f) pseudo-second-order kinetics.

Table 1 Kinetic parameters of GO/CS and RGO/CS nanocomposite hydrogels for three dye removal at 298 K (experimental data obtained from Fig. 5)

		Pseudo-first-order model			Pseudo-second-order model		
		q_e (mg/g)	R^2	k_1 (min^{-1})	q_e (mg/g)	R^2	k_2 (g/(mg min))
CR	GO-CS	10.188	0.7803	0.04835	12.026	0.9973	0.00071
	RGO-CS	12.869	0.6334	0.05858	16.337	0.9925	0.00031
RhB	GO-CS	1.885	0.9892	0.02396	1.974	0.9999	0.02408
	RGO-CS	1.834	0.9920	0.03464	1.913	0.9999	0.03464
MB	GO-CS	3.486	0.9985	0.2994	3.504	0.9999	0.9118
	RGO-CS	3.398	0.9967	0.24715	3.442	0.9999	0.2954

process. At the same time, various spectral results indicate that the organized structure and characteristics of the GO sheets remain mainly unchanged prior and post gelation. The data of adsorption capacity experiments suggest that the prepared 3D GO-based hydrogels can efficiently remove dyes from wastewater in accordance with the pseudo-second-order model. We anticipate that the GO-based composite hydrogels prepared in the present study could open up new avenues for the design and application of composite hydrogels materials.

Received 28 August 2015; accepted 16 September 2015; published online 30 September 2015

1 Novoselov KS, Geim AK, Morozov SV, *et al.* Electric field effect in atomically thin carbon films. Science, 2004, 306: 666–669
2 Geim AK, Novoselov KS. The rise of graphene. Nat Mater, 2007, 6: 183–191
3 Li D, Kaner RB. Materials science-graphene-based materials. Science, 2008, 320: 1170–1171
4 Geim AK. Graphene: status and prospects. Science, 2009, 324: 1530–1534
5 Huang X, Qi X, Boey F, Zhang H. Graphene-based composites. Chem Soc Rev, 2012, 41: 666–686
6 Xu YX, Zhao L, Bai H, *et al.* Chemically converted graphene induced molecular flattening of 5,10,15,20-tetrakis(1-methyl-4-pyridinio)porphyrin and its application for optical detection of cadmium(II) ions. J Am Chem Soc, 2009, 131: 13490–13497
7 Park S, An J, Jung I, *et al.* Colloidal suspensions of highly reduced graphene oxide in a wide variety of organic solvents. Nano Lett, 2009, 9: 1593–1597
8 Kim J, Cote LJ, Kim F, *et al.* Graphene oxide sheets at interfaces. J Am Chem Soc, 2010, 132: 8180–8186
9 Wu S, He Q, Tan C, *et al.* Graphene-based electrochemical sensors. Small, 2013, 9: 1160–1172
10 Geng Z, Lin Y, Yu X, *et al.* Highly efficient dye adsorption and removal: a functional hybrid of reduced graphene oxide–Fe_3O_4 nanoparticles as an easily regenerative adsorbent. J Mater Chem, 2012, 22: 3527–3535
11 Wang MY, Zhu W, Zhang DE, *et al.* CeO_2 hollow nanospheres decorated reduced graphene oxide composite for efficient photocatalytic dye-degradation. Mater Lett, 2014, 137: 229–232
12 Liu F, Chung S, Oh G, Seo TS. Three-dimensional graphene oxide nanostructure for fast and efficient water-soluble dye removal. ACS Appl Mater Interfaces, 2012, 4: 922–927
13 Sereshti H, Samadi S, Asgari S, Karimi M. Preparation and application of magnetic graphene oxide coated with a modified chitosan pH-sensitive hydrogel: an efficient biocompatible adsorbent for catechin. RSC Adv, 2015, 5: 9396–9404
14 Wu JH, Chen AP, Qin M, *et al.* Hierarchical construction of a mechanically stable peptide-graphene oxide hybrid hydrogel for drug delivery and pulsatile triggered release *in vivo*. Nanoscale, 2015, 7: 1655–1660
15 Guo H, Jiao T, Zhang Q, *et al.* Preparation of graphene oxide-based hydrogels as efficient dye adsorbents for wastewater treatment. Nanoscale Res Lett, 2015, 10: 272
16 Zhou WW, Ding CY, Jia XT, *et al.* Self-assembly of Fe_2O_3/reduced graphene oxide hydrogel for high Li-storage. Mater Res Bull, 2015, 62: 19–23
17 Adhikari B, Palui G, Banerjee A. Self-assembling tripeptide based hydrogels and their use in removal of dyes from waste-water. Soft Matter, 2009, 5: 3452–3460
18 Ray S, Das AK, Banerjee A. pH-responsive, bolaamphiphile-based smart metallo-hydrogels as potential dye-adsorbing agents, water purifier, and vitamin B12 carrier. Chem Mater, 2007, 19: 1633–1639
19 Adhikari B, Biswas A, Banerjee A. Graphene oxide-based hydrogels to make metal nanoparticle-containing reduced graphene oxide-based functional hybrid hydrogels. ACS Appl Mater Interfaces, 2012, 4: 5472–5482
20 Biswas A, Banerjee A. Sunlight induced unique morphological transformation in graphene based nanohybrids: appearance of a new tetra-nanohybrid and tuning of functional property of these nanohybrids. Soft Matter, 2015, 11: 4226–4234
21 Adhikari B, Biswas A, Banerjee A. Graphene oxide-based supramolecular hydrogels for making nanohybrid systems with Au nanoparticles. Langmuir, 2012, 28: 1460–1469
22 Xu Y, Wu Q, Sun Y, *et al.* Three-dimensional self-assembly of graphene oxide and DNA into multifunctional hydrogels. ACS Nano, 2010, 4: 7358–7362
23 Tung VC, Kim J, Cote LJ, Huang J. Sticky interconnect for solution-processed tandem solar cells. J Am Chem Soc, 2011, 133: 9262–9265
24 Bai H, Li C, Wang X, Shi G. On the gelation of graphene oxide. J Phys Chem C, 2011, 115: 5545–5551
25 Velmurugan N, Kumar GG, Han SS, *et al.* Synthesis and characterization of potential fungicidal silver nano-sized particles and chitosan membrane containing silver particles. Iran Polym J, 2009, 18: 383–392
26 Jiao T, Zhou J, Zhou JX, *et al.* Synthesis and characterization of chitosan-based Schiff base compounds with aromatic substituent groups. Iran Polym J, 2011, 20: 123–136
27 Krishna Rao KSV, Madhusudana Rao K, Nagendra Kumar PV, Chung ID. Novel chitosan-based pH sensitive micro-networks for the controlled release of 5-fluorouracil. Iran Polym J, 2010, 19: 265–276
28 El Achaby M, Essamlali Y, El Miri N, *et al.* Graphene oxide reinforced chitosan/polyvinylpyrrolidone polymer bio-nanocomposites. J Appl Polym Sci, 2014, 131: 41042
29 Malini M, Thirumavalavan M, Yang WY, *et al.* A versatile chitosan/ZnO nanocomposite with enhanced antimicrobial properties. Int J Biol Macromol, 2015, 80: 121–129
30 Ordikhani F, Farani MR, Dehghani M, *et al.* Physicochemical and biological properties of electrodeposited graphene oxide/chitosan films with drug-eluting capacity. Carbon, 2015, 84: 91–102
31 Ardeshirzadeh B, Anaraki NA, Irani M, *et al.* Controlled release of doxorubicin from electrospun PEO/chitosan/graphene oxide nanocomposite nanofibrous scaffolds. Mat Sci Eng C Mater, 2015, 48: 384–390
32 Chowdhuri AR, Tripathy S, Chandra S, *et al.* A ZnO decorated chitosan-graphene oxide nanocomposite shows significantly enhanced antimicrobial activity with ROS generation. RSC Adv, 2015, 5: 49420–49428
33 Li D, Muller MB, Gilje S, *et al.* Processable aqueous dispersions of graphene nanosheets. Nat Nanotechnol, 2008, 3: 101–105
34 Chen B, Liu M, Zhang L, *et al.* Polyethylenimine-functionalized graphene oxide as an efficient gene delivery vector. J Mater Chem, 2011, 21: 7736–7741
35 Chandra V, Kim KS. Highly selective adsorption of Hg^{2+} by a polypyrrole–reduced graphene oxide composite. Chem Commun, 2011, 47: 3942–3944
36 Bose S, Kuila T, Uddin ME, *et al. In-situ* synthesis and characterization of electrically conductive polypyrrole/graphene nanocomposites. Polymer, 2010, 51: 5921–5928

37 Konwer S, Boruah R, Dolui SK. Studies on conducting polypyrrole/graphene oxide composites as supercapacitor electrode. J Electron Mater, 2011, 40: 2248–2255
38 Du X, Guo P, Song HH, Chen XH. Graphene nanosheets as electrode material for electric double-layer capacitors. Electrochim Acta, 2010, 55: 4812–4819
39 Ferrari AC, Robertson J. Interpretation of Raman spectra of disordered and amorphous carbon. Phys Rev B, 2000, 61: 14095–14107
40 Malard LM, Pimenta MA, Dresselhaus G, Dresselhaus MS. Raman spectroscopy in graphene. Phys Rep, 2009, 473: 51–87
41 Kudin KN, Ozbas B, Schniepp HC, *et al.* Raman spectra of graphite oxide and functionalized graphene sheets. Nano Lett, 2008, 8: 36–41
42 Calizo I, Balandin AA, Bao W, *et al.* Temperature dependence of the Raman spectra of graphene and graphene multilayers. Nano Lett, 2007, 7: 2645–2649
43 Kim KS, Zhao Y, Jang H, *et al.* Large-scale pattern growth of graphene films for stretchable transparent electrodes. Nature, 2009, 457: 706–710
44 Balashov T, Takács AF, Wulfhekel W, Kirschner J. Magnon excitation with spin-polarized scanning tunneling microscopy. Phys Rev Lett, 2006, 97: 187201
45 Akhavan O. Bacteriorhodopsin as a superior substitute for hydrazine in chemical reduction of single-layer graphene oxide sheets. Carbon, 2015, 81: 158–166
46 Sharma A, Kumar S, Tripathi B, *et al.* Aligned CNT/polymer nanocomposite membranes for hydrogen separation. Int J Hydrogen Energy, 2009, 34: 3977–3982
47 Jiao TF, Wang YJ, Zhang QR, *et al.* Regulation of substituent groups on morphologies and self-assembly of organogels based on some azobenzene imide derivatives. Nanoscale Res Lett, 2013, 8: 160
48 Jiao TF, Wang YJ, Gao FQ, *et al.* Photoresponsive organogel and organized nanostructures of cholesterol imide derivatives with azobenzene substituent groups. Prog Nat Sci, 2012, 22: 64–70
49 Jiao TF, Gao FQ, Wang YJ, *et al.* Supramolecular gel and nanostructures of bolaform and trigonal cholesteryl derivatives with different aromatic spacers. Curr Nanosci, 2012, 8: 111–116

Acknowledgements This work was supported by the National Natural Science Foundation of China (21473153 and 21207112), the National Natural Science Foundation of Hebei Province (B2013203108), the Science Foundation for the Excellent Youth Scholars from the Universities and Colleges of Hebei Province (YQ2013026), the Support Program for the Top Young Talents of Hebei Province, the Scientific and Technological Research and Development Program of Qinhuangdao City (201502A006), and the Open Foundation of National Key Laboratory of Biochemical Engineering (Institute of Process Engineering, Chinese Academy of Sciences (CAS)).

Author contributions Jiao T, Zhang Q, and Peng Q designed the project and experiments. Zhao H, Zhang L, Zhou J, and Yan X performed the experiments. Zhao H, Jiao T and Zhang Q analyzed the results and wrote the manuscript with contribution from all authors.

Conflict of interest The authors declare that they have no conflict of interest.

Tifeng Jiao is a professor of applied chemistry at the School of Environmental and Chemical Engineering, Yanshan University. He received his PhD degree in physical chemistry in 2006 at the Institute of Chemistry, CAS. His research focuses on the controlled synthesis, self-assembly, and applications of nanocomposites and nanomaterials.

中文摘要 本文通过壳聚糖分子与氧化石墨烯(GO)的自组装成功制备了GO-壳聚糖复合水凝胶, 并对该水凝胶进行了表征. 研究发现复合水凝胶中存在网状微观结构. 吸附性能结果表明制得的基于GO的复合水凝胶可以有效地从废水中去除三种测试染料分子, 同时符合准二阶模型. 该水凝胶的染料吸附能力主要来源于GO片层, 而壳聚糖分子促进了GO片层的凝胶化过程. 目前的研究结果表明制备的复合水凝胶可以作为良好的吸附剂应用于废水处理以及有害染料去除等领域.